THE ANNALS OF "DUNAREA DE JOS" UNIVERSITY OF GALATI.
FASCICLE IX. METALLURGY AND MATERIALS SCIENCE
N^0. 1 – 2009, ISSN 1453 – 083X

INFLUENCE OF TECHNOLOGICAL PARAMETERS ON THE EVOLUTION OF NICKEL FILMS DEPOSITED BY ELECTROLYSIS

Maria POROCH-SERIŢAN[1], Gheorghe GUTT[1], Maria BOBU[1], Traian SEVERIN[1], Silviu STROE[1], Carmen MIHOC[2]

[1]"Ştefan cel Mare" University of Suceava,
[2] Physics of New Materials, University of Rostock,
email: mariap@usv.ro, g.gutt@usv.ro

ABSTRACT

The influence of technological parameters on the structure of nickel layers electrodeposited on a copper substrate in a Watts bath has been studied. The complex influence of current densities, temperature and pH values on the formation of the deposition layers are compared. The surface morphology of the nickel films was analyzed by scanning electron microscopy (SEM) and atomic force microscopy (AFM). X-ray diffraction (XRD) was used to investigate the crystallinity of the prepared samples. The increase in the current density leads to fine crystallized films, while layers obtained at even higher current density have dendritic structures. The temperature increasing results in a structure change from fine to coarse.

KEYWORDS: *nickel electrodeposition, current density, temperature, pH, Watts bath*

1. Introduction

Electroplated nickel is used extensively in many engineering applications, ranging from simple thin film for decorative purposes and corrosion- and wear-resistant coatings to bulk electroformed products **[1]**. Although electroplated nickel has been widely used for over a century now, considerable interest remains in improving its mechanical, electrical, magnetic and corrosion properties. These properties are dependent on surface structure (preferred orientation and grain size) of deposits, which can be substantially influenced by the deposition parameters **[1-7]**.

The size of the crystallite grains is directly correlated with the ratio between the nucleation rate and the growing speed of the crystals already formed. If many the crystallite grains are formed in unit of time, the size of the grains in the metallic deposition will be lower **[8]**.

The surface structure of deposits depends of the number of formed germs during the electrolysis and the ion concentration decrease at the deposited layer/electrolyte interface (ion diffusion rate). The deposition crystallites structure is strongly affected by the technological parameters that influence the ions concentration in the cathodic layer **[9]**. This paper presents the influence of the technological parameters on the structure of a nickel layer electrodeposited on a copper substrate using a Watts bath.

2. Experimental details

2.1. Apparatus and materials

Nickel electrodeposition was carried out in a rectangular cell of size 13.9 cm x 12.5 cm x 10 cm made from Plexiglas, which corresponds to a volume of 1.75 l. The cathode [made by 99.98% purity copper, having the following dimensions (h x L x l): 8.0 cm x 9.8 cm x 0.1 cm] and the anode [made by 99.7% purity nickel, having the following dimensions (h x L x l): 10.0 cm x 4.0 cm x 0.3 cm] were fixed in the electrolysis cell in such a way that the surface immersed in electrolyte was the following: 0.6 dm^2 and respectively 0.25 dm^2.

The cathode surface was prepared in advance for each electrodeposition experiment, according to the literature procedure **[9]**.

2.2. Reagents

The nickel electrolyte of Watts bath type **[10]**, with composition shown in Table 1 was prepared from pure technical reagents (nickel sulphate, nickel chloride and boric acid) purchased from

INDUSTRIALCHIM, Bucharest. The diluted solution of sodium hydroxide (NaOH) was used to adjust the pH electrolyte at value of 3.0; 4.0; 5.0 and 6.0. All solutions were prepared with distilated water.

Table 1. *The chemical composition of Watts electrolytic bath for nickel electroplating*

Chemical composition	Quantity (g/L)
Nickel chloride, $NiCl_2 \cdot 6H_2O$	40.5
Nickel sulphate $NiSO_4 \cdot 6H_2O$	292.5
Boric acid, H_3BO_3	31.5

2.3. Electrolysis

For each experiment were used 2400 Coulomb of electricity by applying current from a regulated power supplier (0 - 18 V, 0 - 10 A, d.c. power supply GWINSTEK GPR-1810HD). A thermostatic water bath (Lauda E100) was used for maintaining invariable the electrolyte temperature. After electrolysis, the cathode and anode were removed from the cells and thoroughly washed with water and dried. The cathodic and anodic respectively current efficiency were calculated from the weight gained by the electrodes following electrolysis.

2.4. Deposit examination

The morphology of the deposits after drying was observed with a scanning electron microscope (SEM, VEGA II LMU - Tescan, Czech Republic) at Faculty of Food Engineering – Suceava, Romania.

Upon the completion of the experiment, surface morphology of nickel deposits were characterized by atomic force microscopy (Scanning Probe Microscope – SPM - SOLVER) at Institute of Physics, Rostock, Germany.

The structure analysis of nickel deposits in order to determine their preferred crystal orientations were made by X-ray diffraction in θ - 2θ configuration, with a Bruker AXS diffractometer (CuKα radiation, λ = 1.54184 Å) at Institute of Physics, Rostock, Germany.

3. Results and discussions

3.1. Effect of the current density on the microstructure

The mechanism of nickel electrodeposition involves surface adsorption of species formed in the cathode film accompanied by inhibition of growth for certain crystal faces.

A survey of the reaction mechanism, as well as the kinetics of nickel electrodeposition from different baths, was given by Saraby-Reintjes and Fleischmann **[11]**.

The generally accepted mechanism involves two consecutive one-electron charge transfers, and the participation of an anion with the formation of an adsorbed complex. This mechanism can be represented as:

$$Ni^{2+} + X^- \rightarrow NiX^+ \quad (1)$$

$$NiX^+ + e^- \rightarrow NiX_{ads} \quad (2)$$

$$NiX_{ads} + e^- \rightarrow Ni + X^- \quad (3)$$

The anion X^- has been variously assumed to be OH^-, SO_4^{2-} or Cl^- **[11-12]**.

Valuable information has been obtained from transient electrochemical techniques. Amblard et al. **[13]** have shown that chronoamperometry is a useful tool to investigate nucleation and growth kinetics. The initial stage of nickel formation was explained in terms of three-dimensional nucleation **[14]**. Additional investigation by means of transmission electron microscopy showed that growing centers have a hemispherical shape due to a radial multiple twinning processes **[15]**. Depending on conditions, morphology, compactness and grain size varied.

The current density plays an important role on the grain size of electrodeposited coatings. In general, high current densities promote the grain refinement **[2-6]**. An increase in the current density results in a higher overpotential that increases the nucleation rate **[16]**. Moreover, when the current density increases, the cluster density can be increased **[17]**.

Scanning electron microscopy micrographs of the nickel deposits obtained for two current densities of J = 1.7 A/dm^2 and J = 5 A/dm^2 respectively, in Watts bath at different technological parameters pH = 4, at T = 45 °C and pH = 6, at T = 15 °C respectively, are shown in Figures 1a-b, 2a-b. The coatings appear compact and homogeneous. Nevertheless the nickel coatings obtained in Watts bath at same conditions of pH and temperature for different current densities have different shape and grain size. The surface morphology of nickel coatings obtained at J = 1.7 A/dm^2 is different compared with the surface morphology obtained at J = 5 A/dm^2.

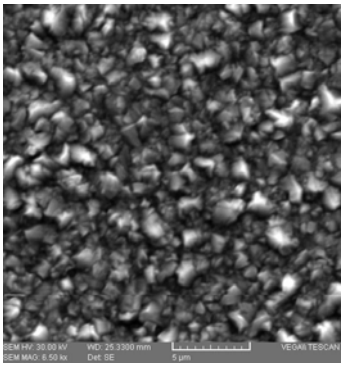
a)
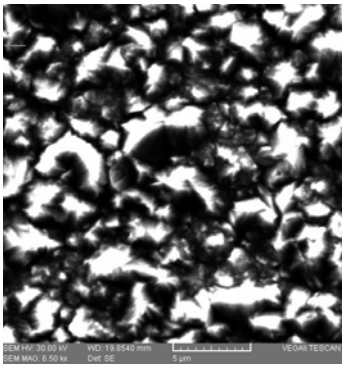
b)

Fig 1. *SEM surface morphology of Ni electroplating in Watts bath at pH = 4, T = 45°C and different value of current density:* ***a)*** *J = 1.7 A/dm^2,* ***b)*** *J = 5 A/dm^2 (SEM, HV = 30.00 kV, MAG = 6.50 kx, Det. SE)*

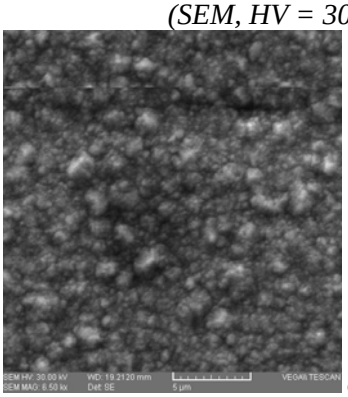
a)
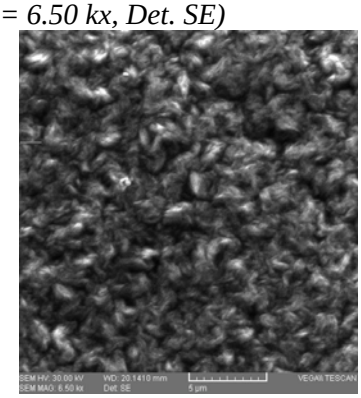
b)

Fig 2. *SEM surface morphology of Ni electroplating in Watts bath at pH = 6, T = 15°C and different value of current density:* ***a)*** *J = 1.7 A/dm^2,* ***b)*** *J = 5 A/dm^2 (SEM, HV = 30.00 kV, MAG = 6.50 kx, Det. SE)*

From Figure 1a it can be seen that when the current density is J =1.7 A/dm^2, the surface morphology of the nickel layer is composed of many large (0.5–1 μm) pyramidal-shaped crystallites and a few fine grains at its surrounding. This pyramidal growth is a typical way of field-oriented texture, that is, the preferential growth in the direction of electric field **[18]**. The Ni deposited at the current density of J = 1.7 A/dm^2 in Watts bath at pH = 6, at T = 15 °C (Figure 2a), appears to have a "cauliflower" structure, that consists in nodular crystallites of non-uniform size with some depressions containing relatively smaller nodular growth.

The Ni layer deposited at the current density of J = 5 A/dm^2 (Figure 1b and 2b, respectively), appeared to consist of areas with very small single grains as well as of areas with grain agglomerates.

At the lowest current density investigated, the grain size was observed to be considerably smaller than for the layers deposited at current densities of J = 5 A/dm^2 and higher. However, when depositing at the lowest current density a mixture of larger grains among small grains tends to develop in the outer layers.

According to general patterns presented by Winand **[2-4]** and Dini **[5]** it is expected that the grain size of the deposits decreases by increasing the current density. The experimental results indicated that the grain size of the coatings increases with increasing current density, it reaches a maximum, then it decreases and deposit structure becomes increasingly fine. The increase in the crystallite size associated by increasing the current density has also been reported in direct current electrodepositions of nickel from other bath types **[7]**, **[19-23]**. Cziráki et al. **[22]** the increase in the grain size at relatively high current densities was attributed to a decrease in the concentration of Ni ions at the deposit–electrolyte interface. Ebrahimi et al. **[19]** suggested that this phenomenon can be attributed to the co-deposition of hydrogen at the cathode interface. The changes in the surface energy and growth mechanisms in the presence of hydrogen are responsible for the increase in the crystallite size by increasing of current density **[19]**. Moreover, based on electrocrystallization consideration, it is possible to indicate that the deviation

from general relationship could be attributed to the difference of kinetic parameters in different baths.

3.2. Effect of the deposition temperature on the microstructure

The influence of the deposition temperature on the microstructure is not treated directly in the Winand diagram **[3]**.

Nevertheless, higher temperatures can be expected to result in a less adsorption of possible inhibitors, thereby enhancing the diffusion and accelerating the reaction speeds.

The influence of a higher temperature is often observed to result in a larger grain size **[5]**.

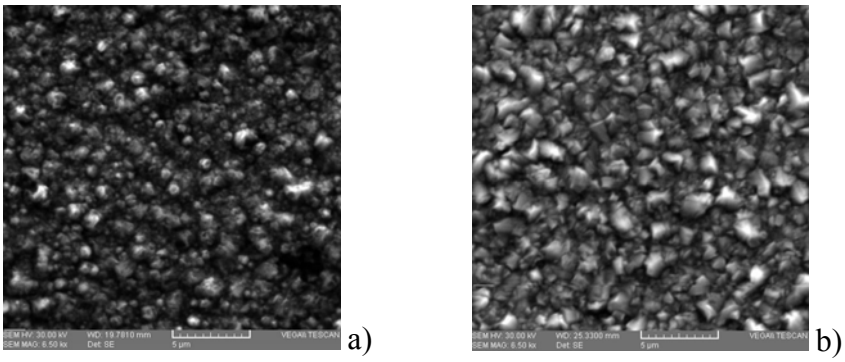

a) b)

Fig 3. *SEM surface morphology of Ni electroplating in Watts bath at pH = 4, J = 1.7 A/dm^2 and different value of temperature:* ***a)*** *T = 15 °C,* ***b)*** *T = 45 °C (SEM, HV = 30.00 kV, MAG = 6.50 kx, Det. SE)*

In Figures 3a and 3b the SEM images of Ni electroplating in Watts bath at pH = 4, current density of J = 1.7 A/dm^2 and deposition temperatures of T = 15 °C and T = 45 °C respectively are compared. Increasing the temperature of electrolyte at T = 45 °C increased the grain size and number of pyramidal-shaped crystallites gradually increased (Figure 3b).

3.3. Effect of pH on the microstructure

In the absence of organic additives, species like H_2, H_{ads} and $Ni(OH)_2$, that form as a result of the reduction of hydrogen ions, determine most of the microstructural features of the nickel deposit.

Electrodeposition of nickel involves a significant amount of hydrogen co-evolution, which may, in part, be incorporated within the deposit. This results in the electrodeposited material being very brittle **[24]**. To avoid this drawback, less acidic solutions can be used. However, Cooper et al. **[25]** have shown that the local pH increases significantly during electrolysis. The local pH change is a major limiting factor for electrolysis at high current density. Nickel oxide or hydroxide is formed at the electrode surface and perturbs the nickel deposition. Indeed, it is known that the stability of $Ni(OH)_2$ is very high **[26]**. As a result, the overall deposition process is irreversibly rendered.

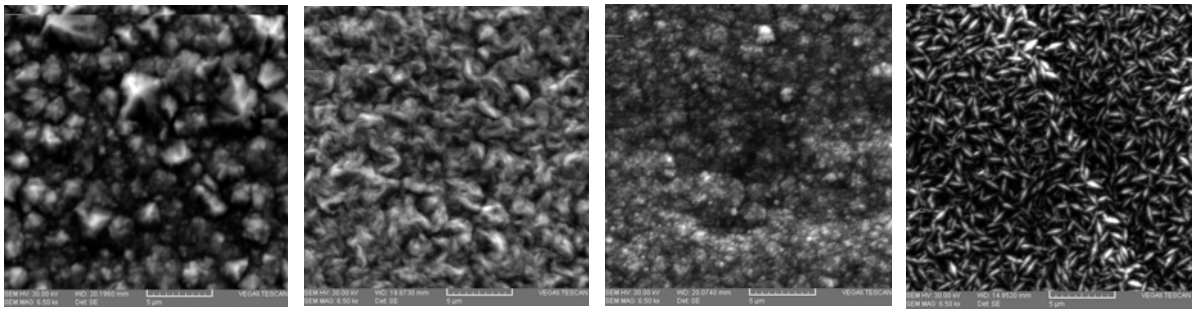

a) b) c) d)

Fig. 4. *SEM surface morphology of Ni electroplating in Watts bath at J = 3.3 A/dm^2, T = 30 °C, time = 20 min. and different value of pH:* ***a)*** *pH = 3,* ***b)*** *pH =4,* ***c)*** *pH =5* ***d)*** *pH =6 (SEM, HM = 30.00kV, MAG = 6.50 kx, Det. SE)*

In Figures 4 are presented the SEM images of nickel coatings obtained in Watts bath at different pH of: pH = 3 (Figure 4a), pH = 4 (Figure 4b), pH = 5 (Figure 4c) and pH = 6 (Figure 4d) respectively. As it can be seen in figure 4a, the obtained layer presents areas with small grain sizes as well as areas with large grain sizes (see the top left corner) of pyramidal-shaped crystallites. At a pH value of 4 (Figure 4b) the layer surface has a fine grains surface. One reason of grain refinement may be that, a large number of hydrogen evolved on the cathode surface, resulted in dramatic increase of pH of nickel deposit/electrolyte interface, thereby enhanced the adsorption and co-deposition of some insoluble material (such as hydroxide nickel) on the cathode surface. The adsorption or incorporation of these insoluble substances at the active growth sites of the crystal will inhibit the growth of crystals, and then finer grained structure will be obtained **[27]**. When the pH value is increased to 5 (Figure 4c) the formation of a coarse-grained structure could be observed. A further increase of the pH value to 6, (Figure 4d), leads to the formation of the polycrystalline Ni which showed a rather regularly branched structure with extended acicular 2–5 μm length crystallites.

Note that in comparing Figures 4a, b, c and d showed that the structure and texture of Ni deposited from Watts bath at current density of J = 3.3 A/dm^2, at T = 30 °C, in 20 minutes is mainly influenced by the solution pH, due to the complex mechanism of nickel electrodeposition, which was studied by various researchers **[28-33]**.

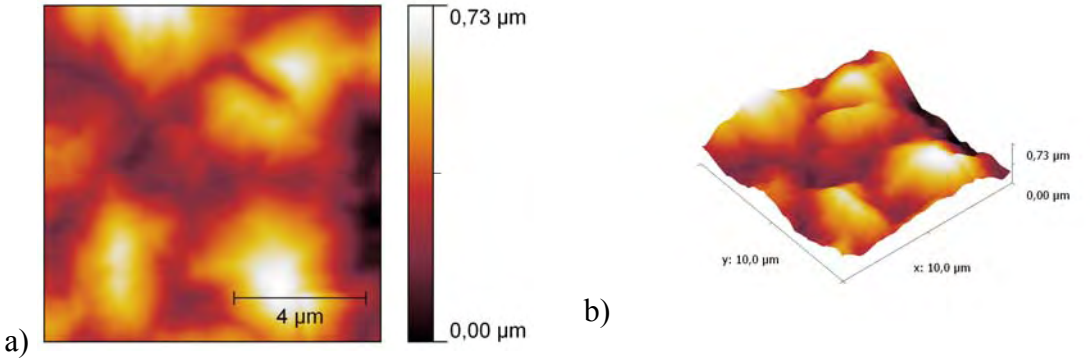

Fig. 5. *AFM micrographs of Ni electroplating in Watts bath at pH = 4, J = 1.7 A/dm^2 at T = 15 °C*

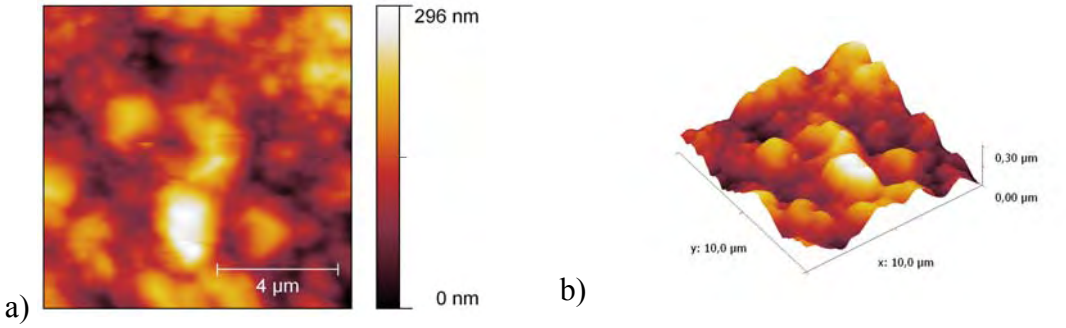

Fig. 6. *AFM micrographs of Ni electroplating in Watts bath at pH = 4, J = 5 A/dm^2 at T = 45 °C*

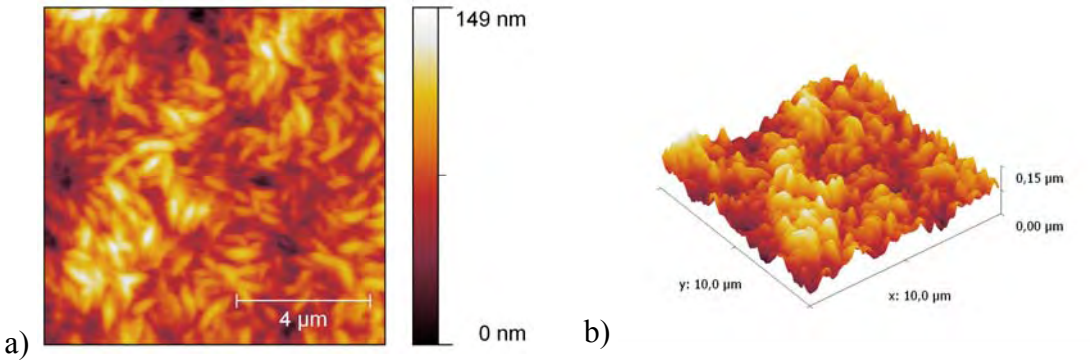

Fig. 7. *AFM micrographs of Ni electroplating in Watts bath at pH = 6, J = 5 A/dm^2 at T = 45 °C*

Figures 5, 6 and 7 show the AFM micrographs and surface local height images of the nickel layers, acquired by contact mode in air counted on 10 μm x 10 μm. The layers were prepared using different electrolysis conditions. The results showed that the performance of nickel electrodeposits is related to their microstructure (such as grain size, surface morphology and crystal orientation). The microstructure is given by the electroplating conditions and composition of the plating bath.

The surface of the nickel coating deposited at pH = 4, J = 1.7 A/dm^2, at T = 15 °C is seen in Figure 5. The size and width of the grains vary throughout the surface. The tri-dimensional image seen in Figure 5b reveals a rough but relatively homogeneous coating. The dark areas in Figure 5a represent the substrate and the bright areas represent the deposited layer.

When the current density and the electrolyte temperature were increased (J = 5 A/dm^2, T = 45 °C) and pH of 4 for the Watts bath was used the layer surface resulted in a smaller grain size of the nickel coating, as seen in Figures 5 and 6. The AFM image clearly shows that the nickel grains still vary in size and shape. Some nanometer sized agglomerates can be observed in Figure 6b.

The experimental results indicate that the grain size increases with increasing current density, it reaches a maximum, and then becomes smaller and the deposit structure becomes increasingly fine. Moreover, the increased temperature favors the depositions in the same sense. The tri-dimensions image seen in Figure 6b shows that the height of the individual grains varies and the largest grains seen in the deposit are 0.30 μm above the surface.

At bath pH of 6, grain size reduction in the nickel coatings can be observed. The AFM tri-dimensional image (Figure 7b) shows the overall small grain size and surface morphology of this coating. Comparison of this deposit with the previous coatings shows that nickel grains are smaller at pH 6.

The effect technological parameter indicated in note on the crystallographic orientations of electrodeposited nickel obtained from Watts bath was examined using X-ray diffraction. Figure 8 shows the XRD spectra for samples deposited at different pH, temperatures and applying different current densities. It can be seen that all electrodeposited samples are epitaxial and the lattice is face-centered cubic (fcc), the same as the Cu substrate which acts as a seed crystal. The Ni crystals grew in the direction of the (111), (200) and (220) planes.

There is however small differences in the crystallization rate with changing the deposition parameters. By changing the pH values (Figure 8b, c) one can see a stronger Ni (111) signal for a smaller pH value and no peak from the Cu substrate. Increasing the pH, the Cu substrate can also be seen. By decreasing the temperature and current density the peaks are wider and smaller which suggests, as expected, a smaller crystallization rate.

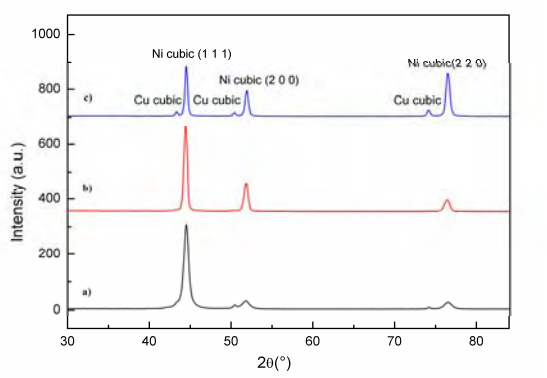

Fig. 8. *XRD patterns showing the influence technological parameter on the crystal orientation of nickel deposits: Note:*
a) *pH = 4, J = 1.7 A/dm^2 at T = 15 °C,*
b) *pH = 4, J = 5 A/dm^2 at T =45 °C,*
c) *pH = 6, J = 5 A/dm^2 at T =45 °C*

4. Conclusions

The influence of technological parameters on the structure of nickel layers electrodeposited on copper substrates using a Watts bath has been studied. The complex influence of current densities, temperature and different bath pHs on the formation of the deposition layers are compared.

The coatings appear compact and homogeneous.

The surface morphology of nickel deposit was analyzed by scanning electronic microscopy (SEM) and atomic force microscopy (AFM).

The results showed that the structure of nickel deposits is influenced by current density and temperature. The increasing current density contributes to the fine crystallized deposits, but deposits obtained at the much high current density have dendritic structures.

At the lowest current density, the grain size appears to be considerably smaller than for the layers deposited at current densities of J = 5 A/dm^2 and higher. However, when depositing at the lowest current density a mixture of grain agglomerates among small grains tends to develop in the outer layers.

The temperature increase determines a change in the layer structure from fine to coarse. Increasing the temperature of electrolyte to T = 45 °C increases the grain size and the number of pyramidal-shaped crystallites gradually increases.

At a pH value of 4 the layer surface has a fine grained surface. When the pH value is increased to pH = 5 the formation of a coarse-grained structure can be observed. A further increase of the pH value to 6 leads to the formation of the polycrystalline Ni which shows a rather regularly branched structure with extended acicular 2–5 μm length crystallites.

XRD patterns show an epitaxial growth of the electrodeposited Ni on the Cu substrate. The Ni layer has a face-centered cubic (fcc) lattice. The higher crystallization rate was obtained for the sample deposited at pH = 4, current density of J = 5 A/dm^2 and T = 45 °C.

Our investigations show that controlled electrodeposition parameters allow tailoring both morphological and structural properties of the synthesized nanostuctured thin films corresponding to the requirements of the specific technological applications.

References

[1]. S. Kaja, H.W. Pickering and W.R. Bitler, *Plat. Surf. Fin*. 72 (1986) 58
[2]. R. Winand, *Hydrometallurgy,* 29 (1992) 567,
[3]. R. Winand, *Electrochim. Acta,* 39 (1994) 1091,
[4]. R. Winand, *J. Appl. Electrochem*., 21 (1991) 377,
[5]. J.W. Dini, *Electrodeposition: The Material Science of Coatings and Substrates*, Noyes Publications, 1993,
[6]. J.W. Dini, *Plat. Surf. Finish*., 75 (1988) 11,
[7]. I. Bakony, E. Tóth-Kádár, L. Pogány, Á. Cziráki, I. Gerőcs, K. Varga-Josepovits, B. Arnold, K. Wetig, *Surf. Coat. Tech*., 78 (1996) 124.
[8]. Firoiu C., *Tehnologia proceselor electrochimice*, Editura Didactică şi Pedagogică, Bucureşti, 1983;
[9]. Oniciu, L., Grűnwald, E., *Galvanotehnica*, Editura Ştiinţifică şi Enciclopedică, Bucureşti, 1980
[10]. di Bari G., *Modern Electroplating*, Fourth Edition, Edited by Mordechay Schlesinger and Milan Paunovic © 2000 John Wiley & Sons. Inc, New York, 2000
[11]. A. Saraby-Reintjes, M. Fleischmann, *Electrochim. Acta*, 29 (1984) 557
[12]. P. Allongue, L. Cagnon, C. Gomes, A. Gündel, V. Costa, *Surf. Sci*., 557 (2004) 41.
[13]. J. Amblard, M. Froment, G. Maurin, D. Mercier and E. Trevisan-Pickacz, *Journal of Electroanalytical Chemistry*, 134 (1982) 345.
[14]. E. Trevisan-Souteyrand, G. Maurin, D. Mercier, *Journal of Electroanalytical Chemistry*, 161 (1984) 17.
[15]. G. Maurin, *Growth and Properties of Metal Clusters,* (edited by J. Bourdon), Elsevier, Amsterdam, (1980), p.101.
[16]. W. Schmickler, *Interfacial Electrochemistry*, OUP, Oxford, 1996.
[17]. R. Winand, *Electrochim. Acta*, 43 (1998) 2925.
[18]. H. Fischer, *Electrodepos. Surf. Treat*., 1 (3) (1973) 239.
[19]. F. Ebrahimi, Z. Ahmed, *J. Appl. Electrochem*., 33 (2003) 733.
[20]. K.L. Morgan, Z. Ahmed, F. Ebrahimi, *Mat. Res. Soc. Symp*. 634 (2001) Materials Research Society.
[21]. A.A. Rasmussen, P. Møller, M.A.J. Somers, *Surf. Coat. Tech*., 200 (2006) 6037.
[22]. Á. Cziráki, B. Fogarassy, I. Gerőcs, E. Tóth-Kádár, I. Bakony, *J. Mater. Sci*., 29 (1994) 4771.
[23]. I. Bakony, E. Tóth-Kádár, T. Tarnóczi, L.K. Varga, Á. Cziráki, I. Gerőcs, B. Fogarassy, *Nonstr. Mater*., 3 (1993) 155.
[24]. R. L. Zeller III, U. Landau, *J. Electrochem. Soc*., 137 (1990) 1107.
[25]. J. H. C. Cooper, D. B. Dreisinger and E. Peters, *J. Appl. Electrochem*., 25 (1995) 642.
[26]. C. Q. Cui, J. Y. Lee, *Electrochim. Acta*, 40 (1995) 1953
[27]. V.S. Abdulin, V.I. Chernenko, *Prot. Met*. 18 (6) (1982) 777 (English translation of Zaschita Metallov)
[28]. R. Oriňáková, L. Trnková, M. Gálová, M. Šupicová, *Electrochim. Acta*, 49 (2004) 3587.
[29]. M. Šupicová, R. Rozik, L. Trnková, R. Oriňáková, M. Gálová, *J. Solid State Electrochem*., 10 (2006) 61.
[30]. J.O.M. Bockris, D. Drazic, A.R. Despic, *Electrochim. Acta*, 4 (1961) 325.]
[31]. W.G. Proud, C. Müller, *Electrochim. Acta*, 38 (1993) 405.
[32]. I. Epelboin, M. Joussellin, R. Wiart, *J. Electroanal. Chem*., 119 (1981) 61,
[33]. E. Chassaing, M. Joussellin, R. Wiart, *J. Electroanal. Chem*., 157 (1983) 75.